

Iridium Thioether Chemistry: The Synthesis and Structures of $[\text{IrL}_2][\text{PF}_6]_3$ and $[\text{IrHL}_2][\text{PF}_6]_2$ ($\text{L} = 1,4,7$ -trithiacyclononane) †

Alexander J. Blake, Robert O. Gould, Alan J. Holder, Timothy I. Hyde, Gillian Reid, and Martin Schröder*

Department of Chemistry, University of Edinburgh, West Mains Road, Edinburgh EH9 3JJ

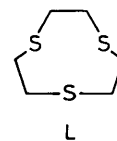
Reaction of $[\{\text{IrCl}(\text{C}_8\text{H}_{14})_2\}_2]$ with 4 molar equivalents of 1,4,7-trithiacyclononane (L) in water-methanol (2:1, v/v) in the presence of HBF_4 affords the iridium(III) hydrido complex $[\text{IrHL}_2]^{2+}$. The complex $[\text{IrHL}_2][\text{PF}_6]_2 \cdot 2\text{MeNO}_2$ crystallises in the monoclinic space group Cc , $a = 19.456\ 0(17)$, $b = 8.152\ 5(9)$, $c = 21.935(3)$ Å, $\beta = 117.008(7)^\circ$, and $Z = 4$. The single-crystal X -ray structure of the complex shows one L ligand bound facially to Ir^{III} , $\text{Ir-S}(1)$ (*trans* to H) 2.476(5), $\text{Ir-S}(4)$ 2.298(5), $\text{Ir-S}(7)$ 2.321(5) Å, with the second L bound as a bidentate ligand through only two S donors, $\text{Ir-S}(11)$ 2.344(5), $\text{Ir-S}(41)$ 2.319(5) Å; the dangling donor $\text{S}(71)$ lies 4.329(6) Å from the iridium centre. The sixth co-ordination site is taken up by a hydride, Ir-H 1.58(6) Å. Treatment of $[\text{IrHL}_2][\text{PF}_6]_2$ with aqueous HNO_3 affords the homoleptic thioether complex $[\text{IrL}_2]^{3+}$. The complex $[\text{IrL}_2][\text{PF}_6]_3 \cdot 5\text{MeNO}_2$ crystallises in the monoclinic space group $C2/c$, $a = 8.581\ 7(13)$, $b = 21.338(4)$, $c = 23.482(7)$ Å, $\beta = 90.94(2)^\circ$, and $Z = 4$. The single-crystal X -ray structure of the complex confirms homoleptic hexathia co-ordination at a centrosymmetric, octahedral iridium(III) centre, $\text{Ir-S}(1)$ 2.342(3), $\text{Ir-S}(4)$ 2.341(3), $\text{Ir-S}(7)$ 2.338(3) Å. The redox properties of $[\text{IrL}_2]^{3+}$ are discussed and compared to those of the rhodium(III) analogue $[\text{RhL}_2]^{3+}$. Spectroelectrochemical measurements using a u.v.-visible optically transparent electrode system confirm the isosbestic and reversible interconversion of $[\text{RhL}_2]^{3+}$, $[\text{RhL}_2]^{2+}$, and $[\text{RhL}_2]^+$.

Our studies on platinum-group metal complexes of 1,4,7-trithiacyclononane (L) have led to the isolation and characterisation of a range of unusual homoleptic thioether complexes of the type $[\text{ML}_2]^{x+}$ ($\text{M} = \text{Ru}, \text{Os}, \text{Rh}, \text{Pd}, \text{or Pt}; x = 2 \text{ or } 3$).¹⁻⁴ However, the synthesis of $[\text{IrL}_2]^{3+}$ has presented particular difficulties due to the high kinetic inertness of the d^6 iridium(III) centre. Attempts to synthesise $[\text{IrL}_2]^{3+}$ from a range of iridium(III) starting materials have led to the isolation of the desired complex in extremely low and unworkable yields.² We argued that an alternative route might be developed involving addition of 2 equivalents of L to $d^8 \text{Ir}^{\text{I}}$ to afford $[\text{IrL}_2]^+$. This highly reactive species, prepared perhaps only *in situ*, could then be oxidised up to the desired d^6 iridium(III) complex $[\text{IrL}_2]^{3+}$. The redox interconversion of d^6 , d^7 , and d^8 metal complexes with L and its N -donor analogue 1,4,7-triazacyclononane has been shown previously for complexes of Pt ,^{2,5,6} Pd ,^{7,8} and Rh ,^{7,9} suggesting that the analogous iridium(III), -(II), -(I) chemistry would be a viable target.

We report herein the high-yield synthesis and structure of the $[\text{IrL}_2]^{3+}$ cation prepared from $[\{\text{IrCl}(\text{C}_8\text{H}_{14})_2\}_2]$. The synthesis and structure of an unusual iridium(III) hydrido complex $[\text{IrHL}_2]^{2+}$ is also described.

Results and Discussion

Reaction of $[\{\text{IrCl}(\text{C}_8\text{H}_{14})_2\}_2]$ with 4 molar equivalents of L in water-methanol (2:1, v/v) under reflux for 16 h under N_2 in the presence of 40% HBF_4 affords a colourless solution from which the complex cation $[\text{IrHL}_2]^{2+}$ can be isolated as a PF_6^- salt in 70% yield. The ^1H n.m.r. spectrum in CD_3CN shows a resonance at $\delta -13.40$ assigned to the metal hydride. In addition, multiplet resonances are observed in the range $\delta 2.6$ – 4.2 (Figure 1) suggesting asymmetric binding of L to the metal centre. This is confirmed by the ^{13}C n.m.r. spectrum which shows six resonances for the methylene C centres of co-ordinated L at 31.35, 35.61, 35.88, 39.01, 39.09, and 40.60 p.p.m.



Fast-atom bombardment mass spectroscopy of $[\text{IrHL}_2][\text{PF}_6]_2$ shows peaks at m/z 699 and 553 assigned to the fragments $[\text{IrHL}_2(\text{PF}_6)]^+$ and $[\text{IrL}_2]^+$ respectively. The i.r. spectrum of $[\text{IrHL}_2][\text{PF}_6]_2$ shows, in addition to bands for co-ordinated L and PF_6^- counter ion, an Ir-H stretching vibration at $2180\ \text{cm}^{-1}$, while elemental analysis confirms the stoichiometry of the product.

Colourless crystals of $[\text{IrHL}_2][\text{PF}_6]_2 \cdot 2\text{MeNO}_2$ were grown by vapour diffusion of diethyl ether into a solution of the complex in MeNO_2 . The single-crystal X -ray structure of the complex confirms (Figure 2) Ir^{III} bound to two L ligands and a hydride ligand. One L is bound facially to Ir^{III} as a tridentate ligand, $\text{Ir-S}(1)$ (*trans* to H) 2.476(5), $\text{Ir-S}(4)$ 2.298(5), $\text{Ir-S}(7)$ 2.321(5) Å, $\text{S}(1)\text{IrS}(4)$ 87.28(17), $\text{S}(1)\text{IrS}(7)$ 87.70(17), $\text{S}(4)\text{IrS}(7)$ 89.81(18)°, with elongation of the $\text{Ir-S}(1)$ bond reflecting the high *trans* influence of hydride ligands. The second L is bound only as a bidentate ligand through two S donors, $\text{Ir-S}(11)$ 2.344(5), $\text{Ir-S}(41)$ 2.319(5) Å, $\text{S}(11)\text{IrS}(41)$ 86.75(18)°. The third S donor is non-bonding with $\text{S}(71)$ lying 4.329(6) Å from the iridium(III) centre; the Ir-H distance is 1.58(6) Å. Relatively few macrocyclic iridium(III) hydride complexes have been prepared.^{2,10,11} The complex $[\text{Ir}(\text{oep})\text{H}]$ ($\text{H}_2\text{oep} = 2,3,7,8,12,13,17,18$ -octaethylporphyrin) is a very useful precursor for the synthesis of the metal-metal bonded dimer, $[\{\text{Ir}(\text{oep})\}_2]$, which activates C-H bonds and O_2 .¹¹ The binding of L as a

† Supplementary data available: see Instructions for Authors, *J. Chem. Soc., Dalton Trans.*, 1990, Issue 1, pp. xix–xxii.

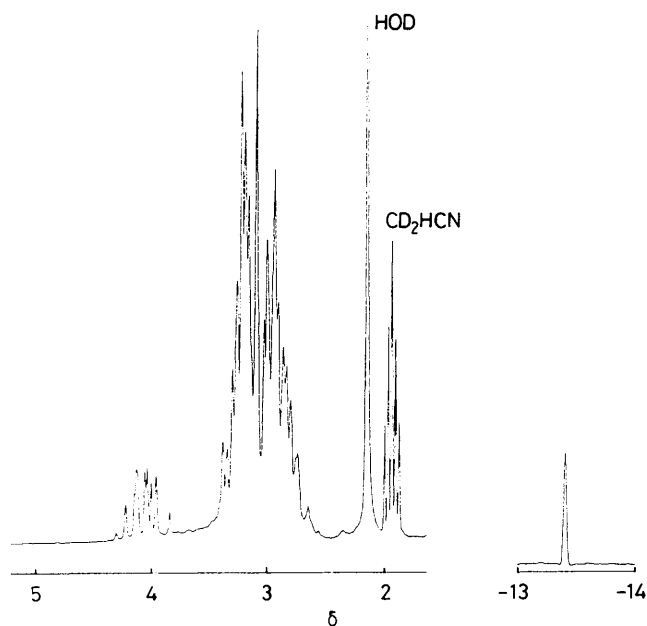


Figure 1. Proton n.m.r. spectrum (80 MHz, CD_3CN , 298 K) of $[\text{IrHL}_2]^{2+}$

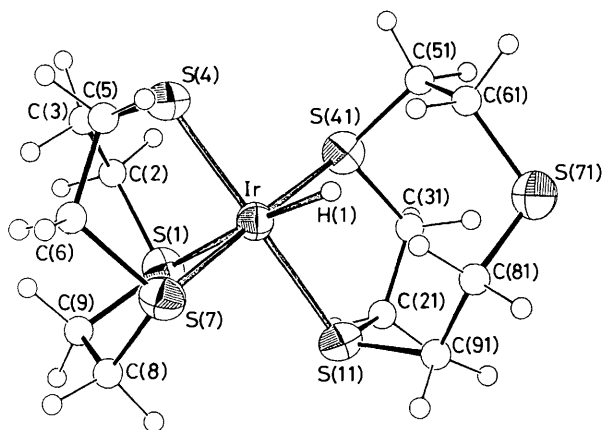


Figure 2. Single-crystal X-ray structure of $[\text{IrHL}_2]^{2+}$ with numbering scheme adopted

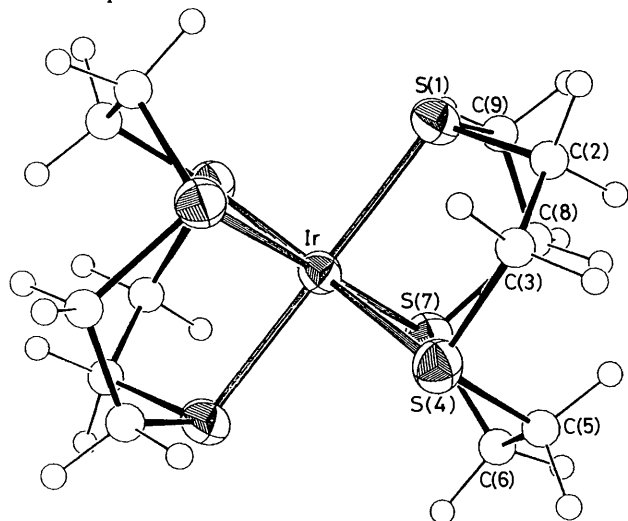


Figure 3. Single-crystal X-ray structure of $[\text{IrL}_2]^{3+}$ with numbering scheme adopted

bidentate ligand to Ir^{III} is particularly interesting. The ligand is pre-organised¹² for facial bonding to transition-metal centres with the three S donors in the metal-free ligand lying in *endo* positions.¹³ Thus, it forms a wide range of very stable octahedral transition-metal complexes in which the minicycle binds facially and acts as a formal six-electron donor to the metal ion.¹ This is similar to the facial binding of arene and pyrazolyborate ligands to metal centres. However, if the electronic properties of the metal centre disfavour facial binding of L, such as for d^8 palladium(II),^{7,14} platinum(II),⁵ gold(III),¹⁵ or d^{10} gold(I)¹⁵ species, bidentate, monodentate, or intermediate co-ordination of L is observed. In the complex $[\text{IrHL}_2]^{2+}$, however, facial binding of L is not disfavoured by the d^6 iridium(III) centre but by the presence of the strongly co-ordinating H^+ ligand.

The complex $[\text{IrHL}_2]^{2+}$ shows an irreversible reduction by cyclic voltammetry at $E_{\text{pc}} = -1.95$ V vs. ferrocene-ferrocenium at -40°C .

Treatment of $[\text{IrHL}_2]^{2+}$ with aqueous HNO_3 under reflux affords $[\text{IrL}_2]^{3+}$ in 75% yield thus transforming the bidentate, four-electron donor L to a tridentate, six-electron donor. The ^1H n.m.r. spectrum of $[\text{IrL}_2]^{3+}$ in CD_3CN shows a symmetric multiplet centred at δ 3.23 as observed for the related complexes $[\text{ML}_2]^{3+}$ ($\text{M} = \text{Co}^{16}$ or Rh^9). No hydrido resonances are observed in the ^1H n.m.r. spectrum of the product. The ^{13}C n.m.r. spectrum shows a single resonance at δ 36.60 p.p.m. Fast-atom bombardment mass spectroscopy of $[\text{IrL}_2][\text{PF}_6]_3$ shows peaks at m/z 843, 697, and 551 assigned to $^{193}\text{IrL}_2(\text{PF}_6)_2^+$, $^{193}\text{IrL}_2(\text{PF}_6) - \text{H}^+$, and $^{193}\text{IrL}_2 - 2\text{H}^+$ respectively. The mass spectroscopic fragmentation pattern suggests that deprotonation of the co-ordinated L ligands occurs during the ionization process. Interestingly, we have recently found that the complexes $[\text{ML}_2]^{3+}$ ($\text{M} = \text{Co}, \text{Rh}, \text{or Ir}$) and related thioether complexes incorporating highly charged metal centres can be deprotonated in solution; this is followed by a ring-opening reaction to afford vinyl thioether complexes.¹⁷

The above, together with elemental analysis and i.r. and electronic spectroscopic data, is consistent with symmetric binding of two L ligands to Ir^{III} in $[\text{IrL}_2][\text{PF}_6]_3$. Single crystals of $[\text{IrL}_2][\text{PF}_6]_3 \cdot 5\text{MeNO}_2$ were grown by vapour diffusion of diethyl ether into a solution of the complex in MeNO_2 . The single-crystal X-ray structure of the complex (Figure 3) confirms homoleptic hexathia co-ordination to Ir^{III} in the centrosymmetric cation, Ir-S(1) 2.342(3), Ir-S(4) 2.341(3), Ir-S(7) 2.338(3) Å, S(1)IrS(4) 88.28(10), S(1)IrS(7) 89.11(10), S(4)IrS(7) 88.46(10)°. The narrow range of Ir-S bond lengths in this compound is as expected for bis(sandwich) complexes of L with d^6 metal centres,^{1,4} with the related d^6 rhodium(III) complex $[\text{RhL}_2]^{3+}$ showing Rh-S(1) 2.331 6(14), Rh-S(4) 2.333 5(12), Rh-S(7) 2.333 5(12) Å, S(1)RhS(4) 88.78(5), S(1)RhS(7) 88.78(5), S(4)RhS(7) 88.84(4)°.⁹

The complex cation $[\text{RhL}_2]^{3+}$ shows two, one-electron reductions by cyclic voltammetry in MeCN at $E_{\frac{1}{2}} = -0.71$ and -1.08 V vs. ferrocene-ferrocenium. These reductions have been assigned to $\text{Rh}^{\text{III}}-\text{Rh}^{\text{II}}$ and $\text{Rh}^{\text{II}}-\text{Rh}^{\text{I}}$ couples respectively. Electrogeneration of the mononuclear d^7 rhodium(II) complex $[\text{RhL}_2]^{2+}$ has been achieved and the metal-radical species identified by e.s.r. spectroscopy.⁹ Clearly, it was important to determine whether the iridium(III) analogue $[\text{IrL}_2]^{3+}$ showed similar redox behaviour.

Cyclic voltammetry of $[\text{IrL}_2]^{3+}$ in MeCN (0.1 mol dm^{-3} NBu_4PF_6) at platinum electrodes shows a reduction at $E_{\text{pc}} = -1.38$ V vs. ferrocene-ferrocenium. This reduction is essentially irreversible down to -40°C . This contrasts with the two reduction processes for $[\text{RhL}_2]^{3+}$ which are reversible under the same conditions. Coulometric measurements obtained by controlled-potential electrolysis at -1.6 V confirm the reduction of $[\text{IrL}_2]^{3+}$ to be a one-electron process.

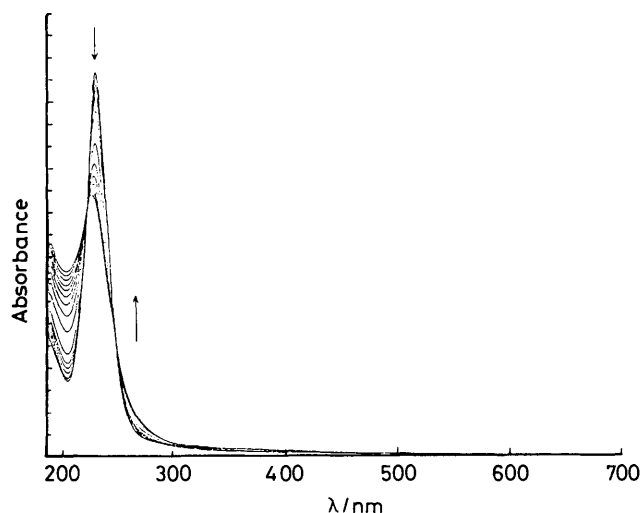


Figure 4. Reduction of $[\text{IrL}_2]^{3+}$ by controlled-potential electrolysis at -1.55 V *vs.* ferrocene-ferrocenium in MeCN (0.1 mol dm^{-3} NBu_4PF_6) at -22°C

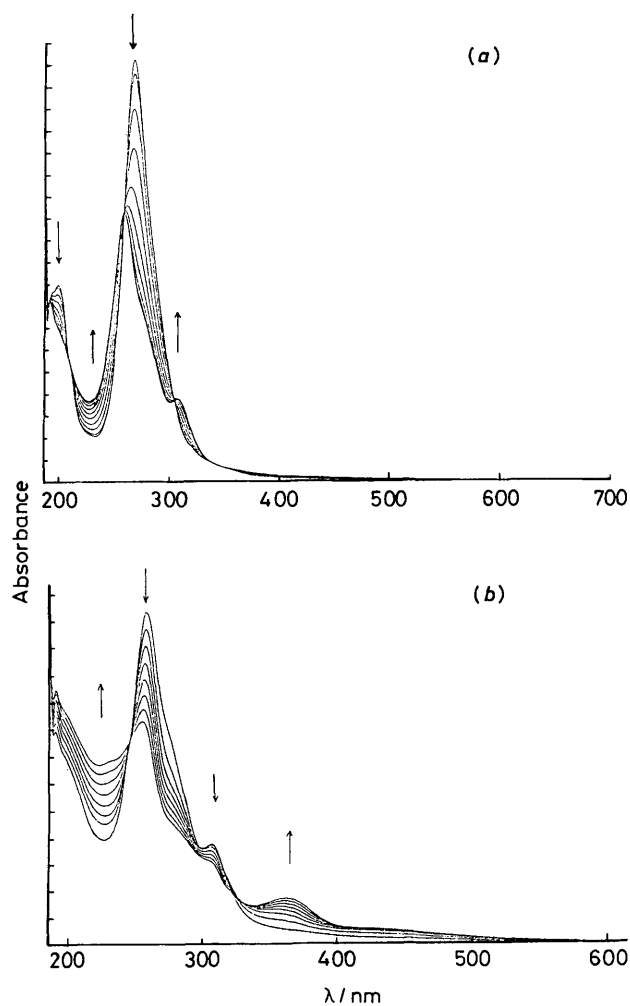


Figure 5. (a) Reduction of $[\text{RhL}_2]^{3+}$ to $[\text{RhL}_2]^{2+}$ by controlled-potential electrolysis at -0.88 V *vs.* ferrocene-ferrocenium in MeCN (0.1 mol dm^{-3} NBu_4PF_6) at -22°C . (b) Reduction of $[\text{RhL}_2]^{2+}$ to $[\text{RhL}_2]^+$ by controlled-potential electrolysis at -1.30 V *vs.* ferrocene-ferrocenium in MeCN (0.1 mol dm^{-3} NBu_4PF_6) at -22°C

However, the reduction product cannot be reoxidised to $[\text{IrL}_2]^{3+}$ on changing the potential to 0.0 V, consistent with the

irreversibility of the reduction wave by cyclic voltammetry. The reduction of $[\text{IrL}_2]^{3+}$ was monitored spectroelectrochemically using an optically transparent electrode system. Figure 4 shows the changes in the electronic spectrum on reduction of $[\text{IrL}_2]^{3+}$ in MeCN at -1.55 V at -22°C . Importantly, the reduction occurs isobestically with loss in intensity and a shift to higher energy of the S→Ir charge-transfer band from $\lambda_{\text{max.}} = 229$ nm, $\epsilon_{\text{max.}} = 25\,000 \text{ dm}^3 \text{ mol}^{-1} \text{ cm}^{-1}$ for the iridium(III) starting material to $\lambda_{\text{max.}} = 225$ nm, $\epsilon_{\text{max.}} = 16\,800 \text{ dm}^3 \text{ mol}^{-1} \text{ cm}^{-1}$ for the reduction product, $\lambda_{\text{iso}} = 248$ and 222 nm. Consistent with the voltammetric and coulometric measurements, reoxidation of the reduction product to the iridium(III) species does not occur up to 0.0 V. No significant paramagnetic signal has thus far been detected by e.s.r. spectroscopy for the reduction product.

These results contrast with spectroelectrochemical measurements on the reduction of $[\text{RhL}_2]^{3+}$ under the same conditions. Figure 5 shows the changes in the electronic spectrum of $[\text{RhL}_2]^{3+}$ on reduction to $[\text{RhL}_2]^{2+}$ at -0.88 V and to $[\text{RhL}_2]^+$ at -1.30 V *vs.* ferrocene-ferrocenium. Reduction of $[\text{RhL}_2]^{3+}$ ($\lambda_{\text{max.}} = 268$ nm, $\epsilon_{\text{max.}} = 30\,600 \text{ dm}^3 \text{ mol}^{-1} \text{ cm}^{-1}$) to $[\text{RhL}_2]^{2+}$ ($\lambda_{\text{max.}} = 307$ and 257 nm, $\epsilon_{\text{max.}} = 6\,200$ and 20 100 $\text{ dm}^3 \text{ mol}^{-1} \text{ cm}^{-1}$) occurs isobestically, $\lambda_{\text{iso}} = 340, 305, 258,$ and 208 nm. As for the iridium system, reduction leads to a loss in intensity and shift to higher energy of the S→M charge-transfer band at 268 nm, consistent with increased electron density at the metal centres. Conversion of $[\text{RhL}_2]^{2+}$ to $[\text{RhL}_2]^+$ ($\lambda_{\text{max.}} = 361$ and 254 nm, $\epsilon_{\text{max.}} = 2\,800$ and 13 500 $\text{ dm}^3 \text{ mol}^{-1} \text{ cm}^{-1}$) also occurs essentially isobestically, $\lambda_{\text{iso}} = 332$ and 246 nm, although the high reactivity of the rhodium(I) species in solution does lead to some decomposition. Cycling between $[\text{RhL}_2]^+$, $[\text{RhL}_2]^{2+}$, and $[\text{RhL}_2]^{3+}$ occurs reversibly and isobestically confirming the ready chemical interconversion of the rhodium(III), -(II), and -(I) complexes.⁹

The porphyrin¹¹ and organometallic¹⁸ chemistry of *d*⁷ iridium(II) species is dominated by binuclear metal-metal bonded species. The cyclic voltammetric, coulometric, and spectroscopic data obtained thus far on the reduction of $[\text{IrL}_2]^{3+}$ are consistent with the formation of such a binuclear iridium(II) species, although this tentative assignment clearly requires further confirmation. Current work is aimed at characterising the redox product(s) of $[\text{IrL}_2]^{3+}$, and monitoring the role of metal-metal bonded species in the reduction of related complexes of Rh^{III} and Ir^{III} with polythia and polyaza macrocyclic ligands.

Experimental

Infrared spectra were measured as KBr and CsI discs using a Perkin-Elmer 598 spectrometer over the range 200–4 000 cm^{-1} . Electrochemical measurements were performed on a Bruker E310 Universal Modular Polarograph. All readings were taken using a three-electrode potentiostatic system in acetonitrile containing 0.1 mol dm^{-3} NBu_4PF_6 or NBu_4BF_4 as supporting electrolyte. Cyclic voltammetric measurements were carried out using a double platinum electrode and a Ag–AgCl reference electrode. All potentials are quoted *versus* ferrocene-ferrocenium. U.v.–visible spectra were measured in quartz cells using a Perkin-Elmer Lambda 9 spectrophotometer. Spectroelectrochemical measurements were carried out in a quartz cell (path length 0.5 mm) fitted with a fine platinum–rhodium gauze as a working electrode. The platinum auxiliary electrode and Ag–Ag⁺ reference electrode were fitted into a quartz extension attached to the cell, and were protected from the bulk solution by porous glass frits. The temperature of the cell was maintained and controlled by the passage of dry, pre-cooled nitrogen gas around the assembly, and monitored using a thermocouple and digital thermometer. Microanalyses were performed by the Edinburgh University Chemistry Department microanalytical

service. E.s.r. spectra were recorded as solids or as frozen glasses down to 77 K using a Bruker ER200D X-band spectrometer. Mass spectra were run by electron impact on a Kratos MS902 and by fast-atom bombardment on a Kratos MS 50TC spectrometer.

Synthesis of $[\text{IrHL}_2][\text{PF}_6]_2$.—Reaction of $[\{\text{IrCl}(\text{C}_8\text{H}_{14})_2\}_2]$ (0.16 g, 0.17 mmol) with L (0.135 g, 0.75 mmol) in refluxing water–methanol (2:1, v/v) (30 cm³) containing 40% HBF_4 (0.5 cm³) for 16 h under N_2 affords a colourless solution. The MeOH was removed *in vacuo* and the aqueous solution extracted with CH_2Cl_2 to remove unreacted L and cyclo-octene. The aqueous solution was reduced to 10 cm³. Addition of an excess of NH_4PF_6 and cooling of the solution afforded a near white product which was recrystallised from MeNO_2 –diethyl ether to give $[\text{IrHL}_2][\text{PF}_6]_2$ as a colourless product in 70% yield (Found: C, 17.2; H, 3.00. Calc. for $[\text{IrHL}_2][\text{PF}_6]_2$: C, 17.1; H, 3.00%). Infrared spectrum: 2 180 cm⁻¹ [$\nu(\text{Ir}-\text{H})$] in addition to bands assigned to L and PF_6^- counter ion. N.m.r. (CD_3CN , 298 K): ¹H (80 MHz), δ -13.40 (s, Ir–H) and 4.2–2.6 (m, CH_2); ¹³C (50.32 MHz), δ 31.35, 35.61, 35.88, 39.01, 39.09, and 40.60 p.p.m. (CH_2). Fast-atom bombardment mass spectrum (3-nitrobenzyl alcohol): *m/z* 699 and 553; calc. for $[\text{IrHL}_2(\text{PF}_6)]^+$ and $[\text{IrL}_2]^+$, 699 and 553 respectively.

X-Ray Structure Determination of $[\text{IrHL}_2][\text{PF}_6]_2 \cdot 2\text{MeNO}_2$.—A colourless columnar crystal (0.2 × 0.25 × 0.6 mm) suitable for X-ray analysis was obtained by vapour diffusion of diethyl ether into a solution of the complex in MeNO_2 .

Crystal data. $\text{C}_{12}\text{H}_{25}\text{F}_{12}\text{IrP}_2\text{S}_6 \cdot 2\text{MeNO}_2$, $M = 965.8$, monoclinic, space group Cc (no. 9), $a = 19.456$ 0(17), $b = 8.152$ 5(9), $c = 21.935$ (3) Å, $\beta = 117.008$ (7)°, $U = 3$ 099.8 Å³ [from 2θ values of 26 reflections measured at $\pm\omega$ (2θ = 29–30°, $\lambda = 0.710$ 73 Å)], $Z = 4$, $D_c = 2.069$ g cm⁻³, $T = 295$ K, $\mu = 4.878$ mm⁻¹, $F(000) = 1$ 888.

Data collection and processing. Stoë STADI-4 four-circle diffractometer, graphite-monochromated Mo- K_α X-radiation, $T = 295$ K, ω –2θ scans with ω scan width (1.05 + 0.347 tanθ)°, 2 250 data measured (2θ_{max}, 45°, $h = -20$ to 20, $k = 0$ –8, $l = 0$ –23), 1 999 unique ($R_{\text{int}} = 0.029$), initial absorption correction by means of ψ scans, giving 1 859 with $F \geq 6\sigma(F)$ for use in all calculations. Slight isotropic crystal decay (ca. 11%) corrected for during data reduction.

Structure solution and refinement. The Ir was found from a Patterson synthesis and iterative cycles of least-squares refinement and difference Fourier synthesis located all non-H atoms. Attempts to solve and refine the structure in the corresponding centric space group ($C2/c$, no. 15) were unsuccessful. At isotropic convergence, final correction for absorption was made using DIFABS.¹⁹ Disorder in one PF_6^- anion was modelled by allowing partial occupation of alternative sites by some F atoms. The Ir, S, P, and fully occupied F atoms were then refined (by least squares on F)²⁰ with anisotropic thermal parameters, with macrocyclic H atoms included at fixed, calculated positions, solvent H atoms as part of rigid groups, and the Ir-bound H refining freely. At final convergence R , $R' = 0.0352$, 0.0422 respectively, $S = 1.077$ for 274 refined parameters. The final ΔF synthesis showed no peak above 0.73 e Å⁻³, the weighting scheme $w^{-1} = \sigma^2(F) + 0.000$ 258 F^2 gave satisfactory agreement analyses, and in the final cycle (Δ/σ)_{max} was 0.31. Although the alternative polarity for the structure gave almost identical residuals and errors on refined parameters, the derived molecular geometry was significantly different: however, a published procedure based on those reflections calculated to be most sensitive²¹ favoured one polarity and all results refer to this. Table 1 gives bond lengths,

Table 1. Bond lengths (Å), angles and torsion angles (°) with estimated standard deviations (e.s.d.s) for $[\text{IrHL}_2][\text{PF}_6]_2 \cdot 2\text{MeNO}_2$

Ir–H(1)	1.58(6)	C(6)–S(7)	1.818(20)
Ir–S(1)	2.476(5)	S(7)–C(8)	1.855(22)
Ir–S(4)	2.298(5)	C(8)–C(9)	1.54(3)
Ir–S(7)	2.321(5)	S(11)–C(21)	1.786(21)
Ir–S(11)	2.344(5)	S(11)–C(91)	1.819(19)
Ir–S(41)	2.319(5)	C(21)–C(31)	1.49(3)
S(1)–C(2)	1.855(19)	C(31)–S(41)	1.849(22)
S(1)–C(9)	1.869(21)	S(41)–C(51)	1.836(21)
C(2)–C(3)	1.47(3)	C(51)–C(61)	1.48(3)
C(3)–S(4)	1.844(19)	C(61)–S(71)	1.819(21)
S(4)–C(5)	1.851(20)	S(71)–C(81)	1.788(21)
C(5)–C(6)	1.56(3)	C(81)–C(91)	1.54(3)
H(1)–Ir–S(1)	173.1(23)	C(3)–S(4)–C(5)	101.8(9)
H(1)–Ir–S(4)	96.5(23)	S(4)–C(5)–C(6)	111.9(13)
H(1)–Ir–S(7)	98.1(23)	C(5)–C(6)–S(7)	113.6(13)
H(1)–Ir–S(11)	84.0(23)	Ir–S(7)–C(6)	102.2(7)
H(1)–Ir–S(41)	84.6(23)	Ir–S(7)–C(8)	106.4(7)
S(1)–Ir–S(4)	87.28(17)	C(6)–S(7)–C(8)	99.2(9)
S(1)–Ir–S(7)	87.70(17)	S(7)–C(8)–C(9)	113.8(14)
S(1)–Ir–S(11)	92.14(17)	S(1)–C(9)–C(8)	112.2(14)
S(1)–Ir–S(41)	89.46(17)	Ir–S(11)–C(21)	107.4(7)
S(4)–Ir–S(7)	89.81(18)	Ir–S(11)–C(91)	112.7(6)
S(4)–Ir–S(11)	178.67(18)	C(21)–S(11)–C(91)	101.4(9)
S(4)–Ir–S(41)	92.06(18)	S(11)–C(21)–C(31)	113.6(14)
S(7)–Ir–S(11)	91.35(18)	C(21)–C(31)–S(41)	115.4(15)
S(7)–Ir–S(41)	176.52(18)	Ir–S(41)–C(31)	101.5(7)
S(11)–Ir–S(41)	86.75(18)	Ir–S(41)–C(51)	114.6(7)
Ir–S(1)–C(2)	102.2(6)	C(31)–S(41)–C(51)	106.7(9)
Ir–S(1)–C(9)	100.9(7)	S(41)–C(51)–C(61)	123.1(15)
C(2)–S(1)–C(9)	102.3(9)	C(51)–C(61)–S(71)	117.3(15)
S(1)–C(2)–C(3)	111.1(13)	C(61)–S(71)–C(81)	105.5(10)
C(2)–C(3)–S(4)	115.2(13)	S(71)–C(81)–C(91)	119.3(14)
Ir–S(4)–C(3)	102.2(6)	S(11)–C(91)–C(81)	120.2(13)
Ir–S(4)–C(5)	105.3(6)		
C(9)–S(1)–C(2)–C(3)	–134.8(13)		
C(2)–S(1)–C(9)–C(8)	63.7(15)		
S(1)–C(2)–C(3)–S(4)	53.6(16)		
C(2)–C(3)–S(4)–C(5)	61.2(15)		
C(3)–S(4)–C(5)–C(6)	–132.1(14)		
S(4)–C(5)–C(6)–S(7)	46.2(17)		
C(5)–C(6)–S(7)–C(8)	67.3(15)		
C(6)–S(7)–C(8)–C(9)	–136.5(15)		
S(7)–C(8)–C(9)–S(1)	49.8(18)		
C(91)–S(11)–C(21)–C(31)	134.6(15)		
C(21)–S(11)–C(91)–C(81)	–76.9(16)		
S(11)–C(21)–C(31)–S(41)	–40.1(20)		
C(21)–C(31)–S(41)–C(51)	–77.5(17)		
C(31)–S(41)–C(51)–C(61)	92.6(18)		
S(41)–C(51)–C(61)–S(71)	–74.4(20)		
C(51)–C(61)–S(71)–C(81)	109.0(16)		
C(61)–S(71)–C(81)–C(91)	–107.2(16)		
S(71)–C(81)–C(91)–S(11)	61.9(20)		

angles, and torsion angles, while atomic co-ordinates appear in Table 2.

Synthesis of $[\text{IrL}_2][\text{PF}_6]_3$.—The complex $[\text{IrHL}_2][\text{PF}_6]_2$ (0.1 g, 0.12 mmol) was dissolved in water (5 cm³) treated with concentrated HNO_3 (1 cm³). The solution was stirred under reflux for 2 h and excess of NH_4PF_6 added to the cooled solution. The white precipitate was collected and washed with small amounts of water and MeOH, and recrystallised from MeNO_2 –diethyl ether to afford $[\text{IrL}_2][\text{PF}_6]_3$ as a colourless product in 70% yield (Found: C, 14.9; H, 2.35. Calc. for $[\text{IrL}_2][\text{PF}_6]_3$: C, 14.6; H, 2.45%). Infrared spectrum: bands assigned to L and PF_6^- counter ion only. N.m.r. (CD_3CN , 298 K): ¹H (80 MHz), δ 3.23 (m, CH_2); ¹³C (50.32 MHz),

Table 2. Atomic co-ordinates with e.s.d.s for $[\text{IrHL}_2][\text{PF}_6]_2 \cdot 2\text{MeNO}_2$

Atom	x	y	z	Atom	x	y	z
Ir	0.0000	0.201 78(6)	0.2500	C(21)	-0.182 9(10)	0.278 3(20)	0.221 4(10)
S(1)	0.028 43(24)	0.097 2(6)	0.365 03(24)	C(31)	-0.167 3(11)	0.250 6(20)	0.227 5(11)
S(4)	0.094 75(25)	0.028 5(5)	0.253 2(3)	C(51)	-0.141 4(11)	0.071 1(21)	0.107 5(10)
S(7)	0.092 1(3)	0.403 3(5)	0.304 0(3)	C(61)	-0.139 8(11)	-0.001 8(21)	0.065 4(10)
S(11)	-0.098 3(3)	0.373 2(6)	0.246 8(3)	C(81)	-0.135 4(11)	0.138 8(20)	0.107 7(10)
S(41)	-0.094 04(25)	0.001 6(5)	0.201 4(3)	C(91)	-0.129 9(10)	0.473 6(21)	0.177 6(9)
S(71)	-0.200 5(3)	0.314 3(6)	0.059 3(3)	F(21)	0.820 6(20)	0.522 2(19)	0.452 0(19)
P(1)	0.139 2(4)	0.216 6(10)	0.080 0(4)	F(22)	0.893 0(15)	0.382(3)	0.494 3(14)
F(11)	0.083 4(17)	0.255(3)	0.102 8(13)	F(23)	0.847 5(15)	0.067(3)	0.382 5(15)
F(12)	0.175 8(9)	0.080 3(18)	0.139 6(8)	F(26)	0.778 1(14)	0.323(3)	0.350 4(14)
F(13)	0.111 2(11)	0.331 3(19)	0.016 5(9)	F(27)	0.886 9(22)	0.366(3)	0.479 1(20)
F(14)	0.213 0(12)	0.186 6(24)	0.066 4(12)	F(28)	0.884 1(20)	0.073(3)	0.456 2(20)
F(15)	0.089 1(9)	0.098 1(15)	0.024 6(8)	F(29)	0.774 (17)	0.202(3)	0.342 7(16)
F(16)	0.192 1(12)	0.342 1(23)	0.134 6(11)	F(210)	0.792 5(18)	0.406(3)	0.405 7(18)
P(2)	0.836 8(3)	0.226 6(7)	0.419 9(3)	O(1S)	0.527 5(15)	0.187 4(22)	0.163 0(12)
F(24)	0.902 9(11)	0.302 3(19)	0.406 2(12)	N(1S)	0.580 3(11)	0.195 0(17)	0.154 3(10)
F(25)	0.771 3(12)	0.146 7(22)	0.434 9(13)	O(2S)	0.644 4(10)	0.176 8(16)	0.201 9(9)
C(2)	0.109 7(10)	-0.045 6(18)	0.383 4(9)	C(1S)	0.572 2(17)	0.219(3)	0.085 3(15)
C(3)	0.104 1(10)	-0.119 0(19)	0.320 3(9)	O(3S)	0.480 7(13)	0.190 5(19)	0.356 0(11)
C(5)	0.185 7(10)	0.146 1(20)	0.296 4(10)	N(2S)	0.417 6(15)	0.204 4(21)	0.360 1(13)
C(6)	0.171 4(10)	0.335 2(19)	0.287 9(10)	O(4S)	0.357 8(14)	0.228 2(21)	0.310 8(12)
C(8)	0.134 8(11)	0.359 9(21)	0.397 1(11)	C(2S)	0.421 9(14)	0.209 5(23)	0.427 6(13)
C(9)	0.078 3(11)	0.359 9(21)	0.419 4(10)	H(1)	-0.029(4)	0.262(4)	0.174(4)

Table 3. Bond lengths (Å), angles and torsion angles (°) with e.s.d.s for $[\text{IrL}_2][\text{PF}_6]_3 \cdot 5\text{MeNO}_2$

Ir-S(1)	2.342(3)	C(3)-S(4)	1.851(11)
Ir-S(4)	2.341(3)	S(4)-C(5)	1.822(12)
Ir-S(7)	2.338(3)	C(5)-C(6)	1.486(17)
S(1)-C(2)	1.826(12)	C(6)-S(7)	1.813(13)
S(1)-C(9)	1.822(12)	S(7)-C(8)	1.824(12)
C(2)-C(3)	1.487(16)	C(8)-C(9)	1.510(17)
S(1)-Ir-S(4)	88.28(10)	Ir-S(4)-C(5)	100.8(4)
S(1)-Ir-S(7)	89.11(10)	C(3)-S(4)-C(5)	101.9(5)
S(4)-Ir-S(7)	88.46(10)	S(4)-C(5)-C(6)	114.4(9)
Ir-S(1)-C(2)	101.6(4)	C(5)-C(6)-S(7)	113.3(9)
Ir-S(1)-C(9)	104.2(4)	Ir-S(7)-C(6)	104.3(4)
C(2)-S(1)-C(9)	102.3(5)	Ir-S(7)-C(8)	100.7(4)
S(1)-C(2)-C(3)	113.3(8)	C(6)-S(7)-C(8)	103.2(6)
C(2)-C(3)-S(4)	111.9(8)	S(7)-C(8)-C(9)	114.7(8)
Ir-S(4)-C(3)	104.0(4)	S(1)-C(9)-C(8)	113.0(8)
C(9)-S(1)-C(2)-C(3)	62.8(9)		
C(2)-S(1)-C(9)-C(8)	-132.5(9)		
S(1)-C(2)-C(3)-S(4)	52.0(10)		
C(2)-C(3)-S(4)-C(5)	-135.7(8)		
C(3)-S(4)-C(5)-C(6)	63.5(10)		
S(4)-C(5)-C(6)-S(7)	49.2(11)		
C(5)-C(6)-S(7)-C(8)	-132.3(9)		
C(6)-S(7)-C(8)-C(9)	64.7(10)		
S(7)-C(8)-C(9)-S(1)	48.5(11)		

δ 36.60 p.p.m. (CH_2). Fast-atom bombardment mass spectrum (3-nitrobenzyl alcohol): m/z 843, 697, and 551; calc. for $[\text{IrL}_2(\text{PF}_6)_2]^+$, $[\text{IrL}_2(\text{PF}_6) - \text{H}]^+$, and $[\text{IrL}_2 - 2\text{H}]^+$, 843, 697, and 551 respectively. Electronic spectrum (MeCN): λ_{max} = 229 nm, ϵ_{max} = 25 000 $\text{dm}^3 \text{mol}^{-1} \text{cm}^{-1}$.

X-Ray Structure Determination of $[\text{IrL}_2][\text{PF}_6]_3 \cdot 5\text{MeNO}_2$.—A colourless, slightly flattened needle ($0.15 \times 0.39 \times 0.58$ mm) suitable for X-ray analysis was obtained by vapour diffusion of diethyl ether into a solution of the complex in MeNO₂.

Crystal data. $\text{C}_{12}\text{H}_{24}\text{F}_{18}\text{IrP}_3\text{S}_6 \cdot 5\text{MeNO}_2$, $M = 1292.8$, monoclinic, space group $C2/c$ (no. 15), $a = 8.5817(13)$, $b =$

$21.338(4)$, $c = 23.482(7)$ Å, $\beta = 90.94(2)^\circ$, $U = 4299$ Å³ [from 20 values of 24 reflections measured at $\pm \omega$ ($2\theta = 29-35^\circ$, $\lambda = 0.71073$ Å)], $Z = 4$ (implying that each Ir lay on a two-fold special position), $D_c = 1.997$ g cm^{-3} , $\mu = 3.608$ mm⁻¹, $F(000) = 2544$.

Data collection and processing. Stoë STADI-4 four-circle diffractometer, graphite-monochromated Mo- K_α X-radiation, $T = 298$ K, $\omega-2\theta$ scans with ω scan width ($1.05 + 0.347 \tan\theta$)², 2914 unique data measured ($2\theta_{\text{max}}$, 45° , $h - 9$ to 9 , $k 0-22$, $l 0-25$), giving 1916 with $F \geq 6\sigma(F)$ for use in all calculations. Slight isotropic crystal decay (ca. 9%) corrected for during data reduction, no absorption correction.

Structure solution and refinement. The position of the Ir on an inversion centre was inferred from cell contents and intensity statistics: subsequent iterative cycles of least-squares refinement and difference Fourier synthesis located all non-H atoms. Disorder in the PF_6^- anions was modelled by allowing partial occupation of alternative sites by some F atoms. Fully occupied non-H atoms were then refined (by least squares on F^2)²⁰ with anisotropic thermal parameters, with macrocyclic H atoms included at fixed, calculated positions and solvent H atoms as part of rigid groups. At final convergence $R, R' = 0.0403, 0.0511$ respectively, $S = 1.047$ for 284 refined parameters, and the final ΔF synthesis showed no peak above $1.31 \text{ e} \text{ \AA}^{-3}$. The weighting scheme $w^{-1} = \sigma^2(F) + 0.00955F^2$ gave satisfactory agreement analyses, a secondary extinction parameter refined to $2.1(4) \times 10^{-8}$, and in the final cycle $(\Delta/\sigma)_{\text{max}}$ was 0.183. Table 3 gives bond lengths, angles, and torsion angles, while atomic coordinates appear in Table 4.

For both structure determinations, atomic scattering factors were inlaid,²⁰ or taken from ref. 22. Molecular geometry calculations utilised CALC²³ and the Figures were produced by ORTEP II.²⁴

Additional material available from the Cambridge Crystallographic Data Centre comprises thermal parameters.

Acknowledgements

We thank the S.E.R.C. for support and Johnson Matthey for generous loans of platinum metals.

Table 4. Atomic co-ordinates with e.s.d.s for $[\text{IrL}_2][\text{PF}_6]_3 \cdot 5\text{MeNO}_2$

Atom	x	y	z	Atom	x	y	z
Ir	0.000 0	0.000 0	0.500 0	O(3S)	0.511 0(20)	0.047 0(10)	0.202 4(8)
S(1)	-0.159 8(3)	0.087 04(13)	0.482 35(12)	N(2S)	0.500 0	0.073 1(19)	0.250 0
C(2)	-0.306 2(13)	0.054 2(6)	0.433 6(5)	C(2S)	0.500 0	0.141 0(14)	0.250 0
C(3)	-0.238 6(12)	0.014 4(5)	0.388 2(4)	O(4S)	0.176 5(24)	0.385 0(7)	0.312 4(7)
S(4)	-0.106 9(3)	-0.046 49(13)	0.417 93(12)	N(3S)	0.245 6(17)	0.383 1(8)	0.270 1(6)
C(5)	0.057 9(13)	-0.041 9(6)	0.370 2(5)	O(5S)	0.317(3)	0.426 2(10)	0.255 3(8)
C(6)	0.141 7(15)	0.019 0(6)	0.371 6(5)	C(3S)	0.254(3)	0.323 6(11)	0.238 9(11)
S(7)	0.190 7(3)	0.045 28(14)	0.443 11(12)	F(13)	0.119(3)	0.177 4(13)	0.208 6(11)
C(8)	0.127 9(14)	0.126 9(5)	0.442 9(5)	F(14)	0.060(3)	0.214 4(11)	0.227 7(9)
C(9)	-0.045 6(15)	0.136 3(5)	0.435 3(5)	F(21)	0.454 6(25)	0.180 4(10)	0.393 2(11)
P(1)	0.000 0	0.149 71(24)	0.250 0	F(22)	0.614(3)	0.212 0(14)	0.456 0(8)
F(11)	0.127 8(11)	0.148 0(5)	0.299 6(4)	F(25)	0.610(5)	0.303 3(18)	0.443 3(19)
F(12)	0.089 6(16)	0.102 1(8)	0.217 7(6)	F(26)	0.587(3)	0.271 7(15)	0.359 8(10)
P(2)	0.517 3(4)	0.248 33(16)	0.409 13(16)	F(27)	0.381(4)	0.225 0(18)	0.370 7(13)
F(23)	0.385 6(16)	0.262 5(8)	0.452 0(6)	F(28)	0.496(4)	0.306 5(15)	0.364 5(13)
F(24)	0.647 0(15)	0.230 5(7)	0.369 1(6)	F(29)	0.487(4)	0.179 6(15)	0.435 5(18)
O(1S)	-0.063 7(17)	0.405 7(6)	0.037 8(7)	F(210)	0.648(4)	0.249 4(22)	0.459 4(13)
N(1S)	0.010 3(16)	0.381 3(6)	0.075 2(7)	F(211)	0.535(5)	0.318 3(16)	0.419 0(19)
O(2S)	0.101 9(16)	0.409 6(7)	0.105 5(7)	F(212)	0.631(6)	0.311 4(19)	0.402 7(22)
C(1S)	-0.008 7(22)	0.313 6(7)	0.084 8(8)				

References

- 1 A. J. Blake and M. Schröder, *Adv. Inorg. Chem.*, in the press.
- 2 M. Schröder, *Pure Appl. Chem.*, 1988, **60**, 517.
- 3 S. R. Cooper, *Acc. Chem. Res.*, 1988, **21**, 141.
- 4 M. N. Bell, A. J. Blake, H.-J. Küppers, M. Schröder, and K. Wiegardt, *Angew. Chem.*, 1987, **99**, 253; *Angew. Chem., Int. Ed. Engl.*, 1987, **26**, 250.
- 5 A. J. Blake, R. O. Gould, A. J. Holder, T. I. Hyde, M. O. Odulate, A. J. Lavery, and M. Schröder, *J. Chem. Soc., Chem. Commun.*, 1987, 118.
- 6 K. Wiegardt, M. Köppen, W. Swiridoff, and J. Weiss, *J. Chem. Soc., Dalton Trans.*, 1983, 1869.
- 7 A. J. Blake, A. J. Holder, T. I. Hyde, Y. V. Roberts, A. J. Lavery, and M. Schröder, *J. Organomet. Chem.*, 1987, **323**, 261; A. J. Blake, A. J. Holder, T. I. Hyde, and M. Schröder, *J. Chem. Soc., Chem. Commun.*, 1987, 987.
- 8 A. J. Blake, L. M. Gordon, A. J. Holder, T. I. Hyde, G. Reid, and M. Schröder, *J. Chem. Soc., Chem. Commun.*, 1988, 1452; A. McAuley, T. W. Whitcombe, and G. Hunter, *Inorg. Chem.*, 1988, **27**, 2634; A. McAuley and T. W. Whitcombe, *ibid.*, p. 3090.
- 9 A. J. Blake, R. O. Gould, A. J. Holder, T. I. Hyde, and M. Schröder, *J. Chem. Soc., Dalton Trans.*, 1988, 1861; S. C. Rawle, R. Yagbasan, K. Prout, and S. R. Cooper, *J. Am. Chem. Soc.*, 1987, **109**, 6181.
- 10 A. J. Blake, T. I. Hyde, and M. Schröder, *J. Chem. Soc., Dalton Trans.*, 1988, 1165.
- 11 See, for example, M. D. Farnos, B. A. Woods, and B. B. Wayland, *J. Am. Chem. Soc.*, 1986, **108**, 3659; K. J. Del Rossi and B. B. Wayland, *J. Chem. Soc., Chem. Commun.*, 1986, 1653; J. P. Collman and K. Kim, *J. Am. Chem. Soc.*, 1986, **108**, 7847.
- 12 R. D. Hancock and A. E. Martell, *Comments Inorg. Chem.*, 1988, **6**, 237.
- 13 R. S. Glass, G. S. Wilson, and W. N. Setzer, *J. Am. Chem. Soc.*, 1980, **102**, 5068.
- 14 K. Wiegardt, H.-J. Küppers, E. Raabe, and C. Krüger, *Angew. Chem.*, 1986, **98**, 1136; *Angew. Chem., Int. Ed. Engl.*, 1986, **25**, 1101.
- 15 A. J. Blake, R. O. Gould, J. A. Greig, A. J. Holder, T. I. Hyde, and M. Schröder, *J. Chem. Soc., Chem. Commun.*, 1989, 876.
- 16 H.-J. Küppers, A. Neves, C. Pomp, D. Ventur, K. Wiegardt, B. Nuber, and J. Weiss, *Inorg. Chem.*, 1986, **25**, 2400.
- 17 A. J. Blake, A. J. Holder, T. I. Hyde, H.-J. Küppers, M. Schröder, S. Stötzel, and K. Wiegardt, *J. Chem. Soc., Chem. Commun.*, 1989, 1600.
- 18 N. Serpone and M. A. Jamieson, in 'Comprehensive Co-ordination Chemistry', eds. G. Wilkinson, R. D. Gillard, and J. A. McCleverty, Pergamon, Oxford, 1987, vol. 4, ch. 49, p. 1097.
- 19 DIFABS, program for empirical absorption corrections, N. Walker and D. Stuart, *Acta Crystallogr., Sect. A*, 1983, **39**, 158.
- 20 SHELX 76, program for crystal structure refinement, G. M. Sheldrick, University of Cambridge, 1976.
- 21 A. J. Blake, R. O. Gould, G. Reid, and M. Schröder, *J. Organomet. Chem.*, 1988, **356**, 389.
- 22 D. T. Cromer and J. L. Mann, *Acta Crystallogr., Sect. A*, 1968, **24**, 321.
- 23 CALC, program for molecular geometry calculations, R. O. Gould and P. Taylor, University of Edinburgh, 1985.
- 24 ORTEP II, interactive version, P. D. Mallinson and K. W. Muir, *J. Appl. Crystallogr.*, 1985, **18**, 51.

Received 11th October 1989; Paper 9/04385C